ENGINEERING RESEARCH JOURNAL (ERJ)

Vol. 1, No. 47 Jan. 2021, pp 14-27

Journal Homepage: http://erj.bu.edu.eg

Performance Enhancement of a Vapour Compression Refrigeration System Using Liquid-Suction Heat Exchanger

E. A. Abdel-Hadi, S. H. Taher, M.R. Salem, and S. A. Eldewiny

Mechanical Engineering Department, Shobra Faculty of Engineering, Benha University

Abstract. The present study investigates experimentally the effect of employing a plain/dimpled internal tube liquid-suction heat exchanger (LSHE). The cycle pressure ratio (P_c/P_{ev}) on the performance of a simple vapour single stage compression refrigeration system using 134a as a working fluid. The LSHE is in vertical position. Through the experiments, the dimples pitch to dimples diameter (λ) is varied in the range of $1 \leq \lambda \leq 4$. While the evaporator pressure (P_{ev}) varied from 1.79 bar to 2.75 bar and condenser (P_c) pressure changed from 13.15 bar to 15.48 bar which gives VCRS pressure ratio between 5.6 and 7.35. The experimental results showed that incorporating a plain or dimpled internal tube LSHE in the system considerably enhances the coefficient of performance (COP). It is evident also that decreasing the dimples pitch ratio augments the COP and the LSHE effectiveness. Furthermore, increasing the pressure ratio considerably improve the COP and the LSHE effectiveness. Finally, empirical correlations are deduced based on the experimental results to calculate the COP and the effectiveness of the LSHE.

Keywords: Experimental, Dimpled tube heat exchanger, Coefficient of performance, Effectiveness.

.

1. INTRODUCTION

The vapour compassion refrigeration system is an important system used in most domestic refrigerators in addition to in numerous large industrial and commercial refrigeration systems [1]. Enhancing the thermal performance of this refrigeration system affects directly on the energy, material and cost savings. There are numerous methods that were employed to improve its COP. Some of these investigated the effect of capillary tube shape and geometrical parameters on the performance [2–8]. In other investigations, the effect of adding nanoparticles to the refrigerant or compressor oil was also examined [9–16]. Another method, which was used in many refrigeration and air conditioning systems is LSHEs, with the basic objective of assuring the entrance of refrigerant in liquid phase to the expansion device. This purpose is achieved by exchanging energy between the cool gaseous refrigerant leaving the evaporator and warm liquid refrigerant exiting the condenser. Klein et al. [17] theoretically examined the influence of employing plain LSHE on vapour compression refrigeration system performance for numerous refrigerants. It was concluded that LSHEs have a minimal pressure loss on the low-pressure side which is useful for systems using R507A, R134a, R12, R404A, R290, R407C, R600, and R410A. Navarro-Esbrí et al. [18] experimentally investigated the performance of a VCRS with and without a LSHE using R22, R134a and R407C as working fluids. A comparison between experimental and theoretical results was reported. It was observed that except for R134a at low pressure ratios, the LSHE adoption showed a positive effect on the COP of the system. Inamdar and Farkade [19] theoretically analyzed the LSHE to examine its effect on the VCRS performance. The effect of LSHE size over a wide range of

operating conditions was presented using of R22, R290, and R134a. The authors concluded that the LSHEs improved the performance of the VCRS for any refrigerant. In addition, the LSHEs increased the temperature and reduced the pressure of the refrigerant entering the compressor causing a decrease in the refrigerant mas flow rate. Inamdar and Farkade [20] experimentally extended their work to investigate the effect of the ambient temperature on the percentage increase in the COP as a result of conducting a plain tube in tube LSHE in the VCRS with using R134a as a refrigerant. During the experiments, the maximum suction and condenser pressures were 2.48 bar and 15.722 bar, respectively. The experiments were performed at different ambient temperatures with and without a LSHE. The results assured that the COP of the system of a LSHE was higher than that of the simple cycle. In addition, the percentage increase in the COP augmented with increasing the ambient temperature.

There are also numerous works that studied the heat transfer and pressure drop characteristics using dimpled tubes as a passive heat transfer enhancement technique. Saleh and Abdel Hameed [21] experimentally examined the flow and heat transfer performance of a dimpled tube heat exchanger of parallel/counter flow configuration. Numerous dimples depths and arrangements (in line and staggered) were tested for Reynolds number ranged from 50 to 3000. It was found that the overall heat transfer rates were 2.5 times greater for the dimpled surface compared to a plain surface and the pressure drop penalties in the range of 1.5 to 2 over plain surfaces. Suresh et al. [22] experimentally tested the thermal performance characteristics of CuO/water nanofluid in a helically dimpled tube. The experiments were done for turbulent flow. It was revealed that the Nusselt number with dimpled tube and nanofluids was 19%, 27% and 39% for 0.1%, 0.2% and 0.3% volume concentrations of nanoparticles in a fluid, respectively. Luki and Ganesan [23] theoretically studied the performance characteristics of a double pipe heat exchanger of internal dimpled tube. A hot flue gas and Al_2O_3/ethyl glycol nanofluid was employed as the working fluids in internal and annulus tubes, respectively. It was observed that the overall heat transfer coefficient and effectiveness of the heat exchanger of dimpled tube were increased by 8% compared to plain tube heat exchanger. Parekh and Chavda [24] experimentally and numerically studied the heat transfer coefficients in a tube of almond dimpled surface for flow Reynolds number range from 25000 to 95000. It was observed that the dimpled tube leaded to higher Nusselt number. In addition, staggered dimple configuration achieved 66% thermal performance factor higher than that of align dimple configuration. Banekar et al. [25] investigated experimentally the hydrothermal performance for almond shape dimpled tube heat exchanger for Reynolds number ranged from 3000 to 6000. The results indicated that a maximum increase in the heat transfer coefficients was 12.7% for the dimple tube when compared with the plain one. In addition, the effectiveness of dimpled tube heat exchanger increased by 22% over the plain tube heat exchanger. Nascimento and Garcia [26] carried out experiments to examine the heat transfer rate in heat exchangers by using shallow square dimples in flat plate tubes. It was observed that the heat transfer was augmented by a factor between 1.37 and 2.28. Ambesange et al. [27] concerned with an experimental set up for augmentation of the forced convection heat transfer over dimpled and without dimple fins. It was observed that dimpled cross sectional circular fins transfer more heat with a high heat transfer coefficient. A maximum increase in heat transfer coefficient in circular fins with dimples of 99.75% was obtained while it was 93.51% without dimpled fins.

From the analysis of the above literature survey, there are numerous studies. It is clear that the LSHE enhances the cycle COP under certain operating conditions. Therefore, the present study aims to show the effect of employing a plain/dimpled internal tube LSHE, in addition to the VCRS pressure ratio on the performance of a simple VCRS based on a single stage compression unit. In the present investigation, the parameters considered here are the LSHE of a plain internal tube, LSHE of a dimpled internal tube (three dimples pitch to dimple diameter ratios), and VCRS pressure ratio.

2. Experimental Setup

The apparatus used in the present investigation comprises of a heating unit and a refrigerant circuit as shown in Fig.1. The heating unit consists of a water tank, electric heaters with a thermostat, pump and the connecting pipes. The refrigerant circuit consists of a compressor,

valves, air cooled condenser, filter drier, sight glass, three capillary tubes, an evaporator, temperature sensors, pressure gauges and the connecting pipes. The evaporator is soft copper tube of 5 m length, 8.3 mm inner diameter and 9.53 mm outer diameter, and is helically coiled. The evaporator is positioned inside the heating tank in vertical position. The refrigerant flows through the evaporator tube while the hot water passes over it. A 1 hp centrifugal compressor model is used; the power consumption is 975 W and output rating cooling capacity is 2066 kcal/hr. Two valves are installed at the compressor inlet and exit; this is used in the charging process. In addition, an air-cooled finned tube condenser with direct-drive propeller fan is used to transfer the thermal energy from the refrigerant to the outdoor air. Three capillary (CAP) tubes of the same length (1.5 m effective length) are employed. These are narrow copper tubes of three different internal diameters;1.4 mm, 1.78 mm and 2.03 mm, respectively. The capillary tubes are coiled with an internal coil diameter of 50 mm.

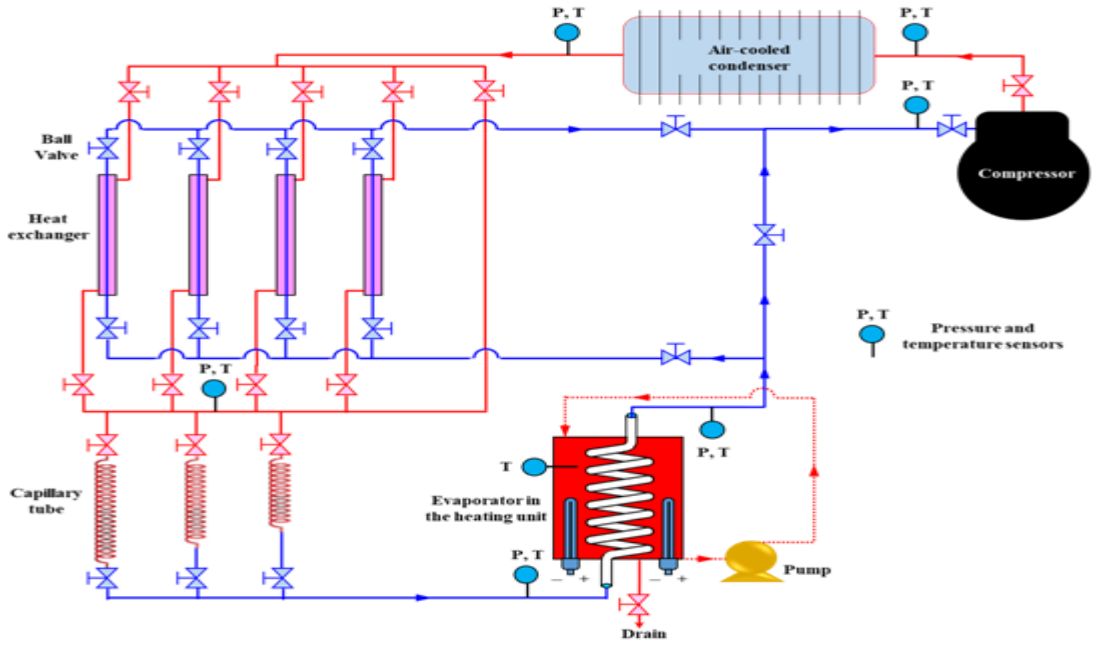

Fig. 1: Schematic diagram of the experimental setup.

Moreover, four concentric tube heat exchangers of counter-flow configuration are constructed and used as LSHEs in the VCRS. One of them is a plain internal tube, while the others have dimpled internal tubes; the dimples are of inline arrangement as indicated in Fig. 2 with different ratios for pitch to dimple diameter (λ) as illustrated in Table 1 and Fig. 3. The annular and internal tubes of the LSHEs are copper tubes of the same length; 500 mm. The inner and outer diameters of the annular pipe of all tested heat exchangers are 16.56 mm and 19.05 mm, respectively. It can be noticed that the internal tubes are filled with fine sand during the dimpling process to prevent any tube buckling, and it then is washed with hot water. Sixteen ball valves are installed before and after the LSHEs to permit the flow of the refrigerant (R134a) through only one of them throughout each experiment.

Fig. 2: A photograph of the dimpled tubes.

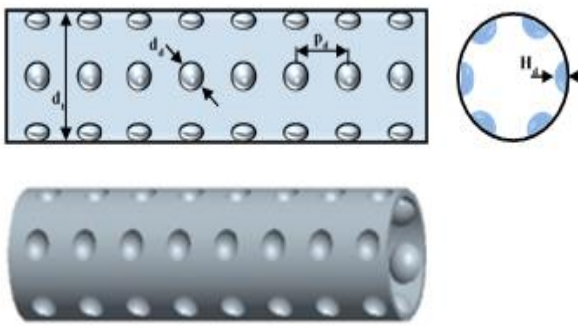

Fig. 3: Hemispherical dimpled tube of inline arrangement.

Table 1: Characteristic dimensions of the internal tube.

Tube No.	$d_{t,i}$ (mm)	$d_{t,o}$ (mm)	d_d (mm)	H_d (mm)	p_d (mm)	λ
1	8.31	9.52	-------			
2			5	0.5	20	4
3					10	2
4					5	1

Six glycerine-filled pressure gauges are fixed to measure the pressures in the VCRS. Three of them are for high pressure up to 260 psi are installed at the inlet and exit of the condenser and the liquid side is in the LSHE. While the other three gauges used for low pressure up to 60 psi, are installed at the inlet and exit of the evaporator and the vapour side of the LSHE. Additionally, eight digital temperature sensors, with a resolution of 0.1°C are used to measure the temperatures of the refrigerant entering or leaving the evaporator, condenser and LSHE. These sensors are fixed on the outer surface of the refrigerant tube. Neglecting the thermal resistance of the copper tube wall, the temperature readings are assumed to be equal to the refrigerant temperatures at these locations. Soft copper tubes of 9.52 mm external diameter and 8.31 mm internal diameter are used for all connections. Furthermore, six copper T-shaped connectors are used to connect the pressure transducers. Furthermore, the electric power consumed by the compressor is calculated through measuring the voltage and current across the compressor by a voltmeter and ammeter of accuracy of ±1% of their readings. The used filter drier and sight glass are of Danfoss type and the size of the inlet and outlet tubes is 3/8 inch.

The heating tank, it is made up of 2 mm thick stainless-steel sheet, which is formed to produce a container with dimensions of 300 mm × 300 mm × 600 mm. There are three holes in the tank; two of them are at the bottom of the tank, used for inlet to the pump and to the drain, while the third port at the top side, is for exit from the pump. Two electric heaters (have a maximum power rating of 6 kW) are fixed horizontally at the bottom of the heating tank to heat the water to the required temperature. The operation of the electric heaters is based on a pre-adjusted digital thermostat, which is used to keep water at constant temperature. Moreover, the outer surface of the tank is thermally insulated with layers of ceramic fiber and glass wool. The heating water is circulated using a 0.5 HP power rating centrifugal pump (with a maximum capacity of 30 l/min). A digital temperature sensor, with a resolution of 0.1°C, is directly inserted into the heating tank to measure the water temperature, while a mercury-in-glass thermometer is used to measure the ambient air temperature.

3. Experimental Procedures

The experimental setup is assembled: the evaporator, compressor, condenser, filter drier, sight glass, capillary tubes, heating tank, pump, piping, valves and the pressure transducers. The temperature sensors are attached on the refrigeration piping at evaporator, heat exchangers, condenser inlet and outlet, in addition to a sensor inserted in the heating tank to measure the heating water temperature. After assembling the VCRS components, it is charged with R134a.

The heating tank is filled with water, and then the electric heaters are turned on. The compressor, condenser fan and pump are turned on. The temperature of the heating water in the tank is adjusted at 20±0.5°C or 30±0.5°C by regulating the temperature of the heating tank through the thermostat. The refrigerant is forced to move through one capillary tube by opening its valve, while the two valves before the other two capillary tubes are closed. The range of the operating conditions are shown in Table 2.

Table 2: Range of operating conditions

Parameter	Range or value
Evaporator heating	20 and 30
Evaporator	$1.79 \leq P_{ev} \leq 2.75$
Condenser refrigerant	$13.15 \leq P_c \leq 15.48$
Condenser to	$5.6 \leq P_c/P_{ev} \leq 7.35$
Dimples pitch to dimple diameter	$1 \leq \lambda \leq 4$

All experiments are conducted in ambient temperature of 28±2°C for three cases; simple, with plain internal tube LSHE, and with dimpled

internal tube LSHE. The steady-state condition has been reached when a maximum variation of 0.5℃ for each temperature sensor reading within 20 minutes is recorded.

4. Data Reduction

The measured temperatures and pressures during the experiments are used to calculate the specific enthalpy of the refrigerant in the different locations of the VCRS. It should be noticed that each experiment is repeated three times, and the average readings of the measured variables are recorded despite the tinny difference between these repeated readings. Microsoft Excel sheets are prepared to process the experimental data for calculating the COP and the other characteristic parameters of the VCRS. The specific enthalpy of the refrigerant is estimated using the measured pressure and temperature at evaporator, LSHE and condenser inlet end exit (locations are named as illustrated in Fig. 4). The estimated specific enthalpies are used for calculating the following parameters:

$$RE = h_1 - h_4 \quad (1)$$

$$w_{com} = h_2 - h_1^* \quad (2)$$

$$q_c = h_2 - h_3 \quad (3)$$

$$COP = \frac{RE}{w_{com}} = \frac{h_1 - h_4}{h_2 - h_1^*} \quad (4)$$

In addition, the superheating of the refrigerant in the evaporator ($\Delta T_{sup,ev}$) and in the LSHE ($\Delta T_{sup,HE}$) are calculated as follows:

$$\Delta T_{sup,ev} = T_1 - T_{ev,ref} \quad (5)$$

$$\Delta T_{sup,HE} = T_1^* - T_1 \quad (6)$$

While, the subcooling of the refrigerant in the condenser ($\Delta T_{sub,c}$) and in the LSHE ($\Delta T_{sub,HE}$) are calculated as follows:

$$\Delta T_{sub,c} = T_{c,ref} - T_3 \quad (7)$$

$$\Delta T_{sub,HE} = T_3 - T_3^* \quad (8)$$

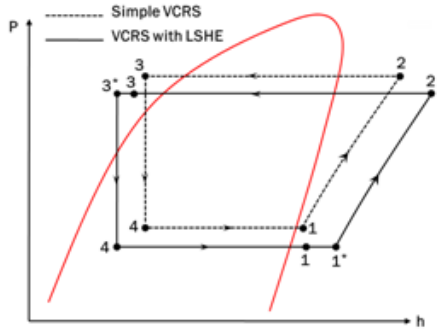

Fig. 4: Schematic representation of the VCRS on the P-h chart.

The specific enthalpy of the R134a entering the evaporator (h_4) is assumed to be equal to the specific enthalpy of the refrigerant entering the capillary tube (h_3^*). To calculate refrigerant mass flow rate in the VCRS, the compressor power is calculated by measuring the voltage drop and current.

$$\dot{m}_{ref} = \frac{W_{com}}{w_{com}} = \frac{IV\ \cos\emptyset}{h_2 - h_1^*} \quad (9)$$

According to Ministry of Electricity and Energy in Egypt, the power factor, $\cos\emptyset$, for the public network is ranged from 0.93 to 0.97; in the present study, it is assumed to be 0.95 [28, 29]. The rate of heat energy transferred through the LSHE between the high and low-pressure refrigerants is calculated as follows:

$$Q_{HE,HP} = \dot{m}_{ref}\,(h_3 - h_3^*) \quad (10)$$

$$Q_{HE,LP} = \dot{m}_{ref}\,(h_1^* - h_1) \quad (11)$$

For no heat loss, $Q_{HE,HP} = Q_{HE,LP}$. Therefore, the percentage error between the LSHE sides with respect to the arithmetical mean of the two ($Q_{HE,ave}$) is calculated as follows:

$$\Delta Q_{HE} = \frac{Q_{HE,HP} - Q_{HE,LP}}{Q_{HE,ave}} \quad (12)$$

Additionally, the LSHE effectiveness (ε_{HE}) is calculated as follows:

$$\varepsilon_{HE} = \frac{T_1^* - T_1}{T_3 - T_1} \quad (13)$$

4.1 Apparatus Validation and Data Verification

The percentage variation in the COP of the VCRS is preferred here for the comparison instead of the COP itself and a comparison is made with those obtained by Inamdar and Farkade [20] which is given as the percentage variation in the COP of the VCRS for operating conditions as illustrated in Table 3. The result of this comparison is shown in Fig. 5.

Table 3: Validation operating conditions.

Parameters	Range or value
Evaporator heating water temperature, °C	20
Ambient air temperature, °C	28, 30, 34 and 38
Evaporator refrigerant pressure, bar	$2.1 \le P_{ev} \le 2.43$
Condenser refrigerant pressure, bar	$15.27 \le P_c \le 15.66$

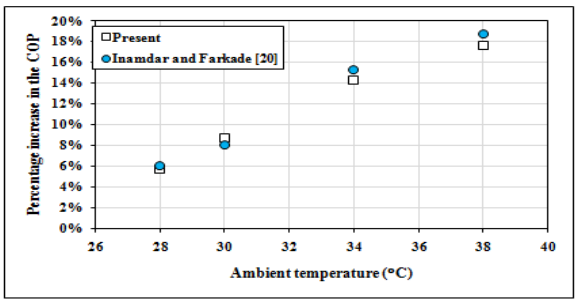

Fig. 5: Validation of the percentage variation in the COP of the VCRS.

It is clear that a fair agreement is noticed between the present results with the published data [20] with a maximum deviation of ±8.75%. This good agreement in comparisons reveals the accuracy of the experimental setup and measurement technique.

5. Results and Discussion

5.1 Effect of LSHE Characteristics on VCRS Operating Conditions

In this analysis, the effect of incorporating a plain or dimpled internal tube LSHE in the VCRS on the cycle operating conditions are investigated. Figure 6 demonstrates these results, while Table 4 summarizes the mean values of the different specifications due to conducting the plain or dimpled internal tube LSHE.

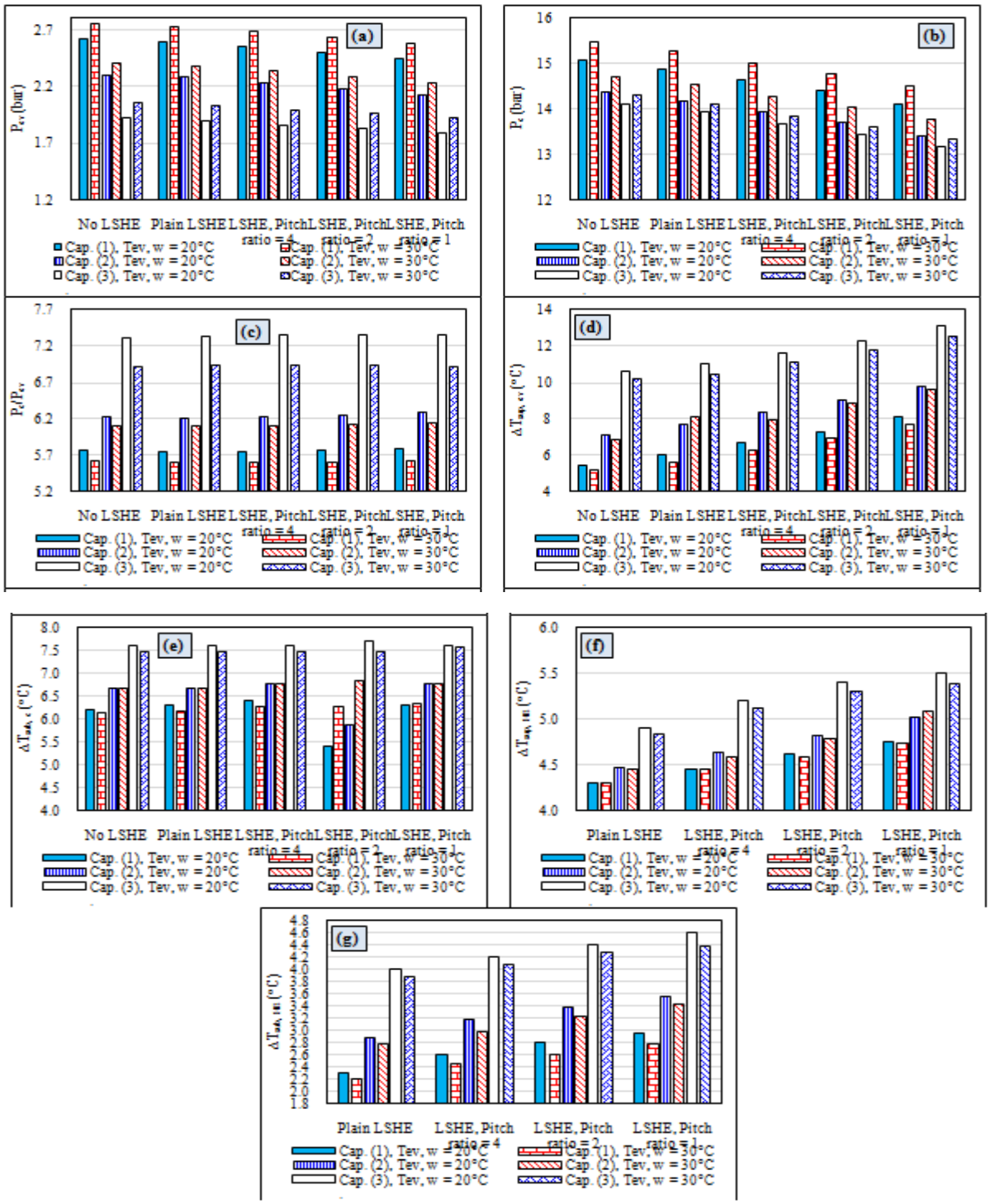

Fig. 6: Effect of LSHE characteristics on VCRS operating conditions; (a) P_{ev}, (b) P_c, (c) P_c/P_{ev}, (d) $\Delta T_{sup,\,ev}$, (e) $\Delta T_{sub,\,c}$, (f) $\Delta T_{sup,\,HE}$, (g) $\Delta T_{sub,\,HE}$.

Table 4: Effect of using the LSHE on the VCRS operating conditions.

Specifications	No LSHE	Plain LSHE	LSHE, λ = 4	LSHE, λ = 2	LSHE, λ = 1
	Average value for all experiments				
P_{ev} (bar)	2.35	2.32	2.28	2.24	2.19
P_c (bar)	14.68	14.5	14.24	14.00	13.73
P_c/P_{ev}	6.33	6.32	6.33	6.34	6.36
$\Delta T_{sup, ev}$ (°C)	7.6	8.2	8.7	9.4	10.1
$\Delta T_{sup, HE}$ (°C)	0	4.5	4.7	4.9	5.1
$\Delta T_{sub, c}$ (°C)	6.8	6.8	6.9	6.7	6.9
$\Delta T_{sub, HE}$ (°C)	0	3.0	3.3	3.5	3.6

It is depicted that incorporating a LSHE in the VCRS affects the operating conditions, where including a plain LSHE reduces the evaporator and condenser mean pressures. This pressure reduction increases with using a dimpled internal tube LSHE. Also the results indicate that this pressure reduction increases with decreasing the dimples pitch ratio. Furthermore, the results demonstrate that the usage of LSHE nearly does not affect the cycle pressure ratio (≅ 6.34) in addition to the amount of subcooling inside the condenser (≅ 6.8°C). In addition, installing the LSHE and decreasing the dimples pitch ratio augments the amount of refrigerant superheating inside both the evaporator and the LSHE, and the amount of refrigerant subcooling inside the LSHE as illustrated in Table 4.

The reduction in the cycle pressures may be due to decreasing λ, which is accompanied by increasing the number of the dimples on the internal tube wall for the same tube diameter and length. This increases the throttling for the tube flow and produces better impingement. In addition, with decreasing the pitch between the dimples, the vortices generation increases on the outer surface (annulus side). This breaks the fluid boundary layers and creates an increase in the pressure drop in both sides of the LSHE, which consequently reduces the cycle pressures and enhances the superheating and subcooling inside the LSHE.

Furthermore, the resulted reduction in the evaporator pressure reduces the corresponding saturation temperature and enhances the latent heat of vaporization of the refrigerant, which permits the increasing in the amount of superheating inside the evaporator. In addition, although the condenser mean pressure slightly decreases, but the amount of subcooling inside the condenser nearly does not vary with installing the plain or dimpled tube LSHE. This may be due to the copper tube connection with the LSHE, which may act as a fin. Accordingly, as the rate of heat exchange in the LSHE is increased, as the subcooling inside the condenser is compensated.

5.2 Effect of LSHE Characteristics on VCRS Specifications

In this analysis, the effect of incorporating a plain or dimpled internal tube LSHE in the system on the system specifications are investigated. Fig. 7 illustrates the obtained results, while Table 5 summarizes the percentage variations of the different specifications due to conducting the plain or dimpled internal tube LSHE.

From Fig. 7 and Table 5, it is indicated that incorporating a plain or dimpled internal tube LSHE in the VCRS considerably affects its specifications. It is clear that including a plain LSHE, the evaporator refrigeration effect, compressor specific work, COP of the VCRS and the condenser heat load extensively increase. Compared with the simple cycle, the average percentage increase in the RE and w_{com} is 9.7% and 3.6%, respectively. This leads to increase cycle COP by 5.9%. While with conducting a dimpled internal tube LSHE, the average percentage increase in the RE and w_{com} is increased with decreasing the dimples pitch ratio by 29.4% and 14%, respectively at λ = 1. This augments the COP by 13.6%. In addition, the effectiveness of the dimpled tube LSHE increases with decreasing the dimples pitch ratio and it is higher than that of the plain tube LSHE by an average percentage of 6.6% and 19.3% at λ = 4 and λ = 1, respectively.

The increase in the RE, q_c and ε_{HE} may be due to increasing the amount of superheating in the evaporator in addition to the amount of superheating and subcooling inside the LSHE, which are increased with decreasing the dimples pitch ratio. Furthermore, the increase in the specific work of the compressor and the reduction in the refrigerant mass flow rate may be due to increasing the refrigerant specific volume at the

compressor inlet as a result of increasing the refrigerant superheating at the compressor inlet with incorporating the LSHE.

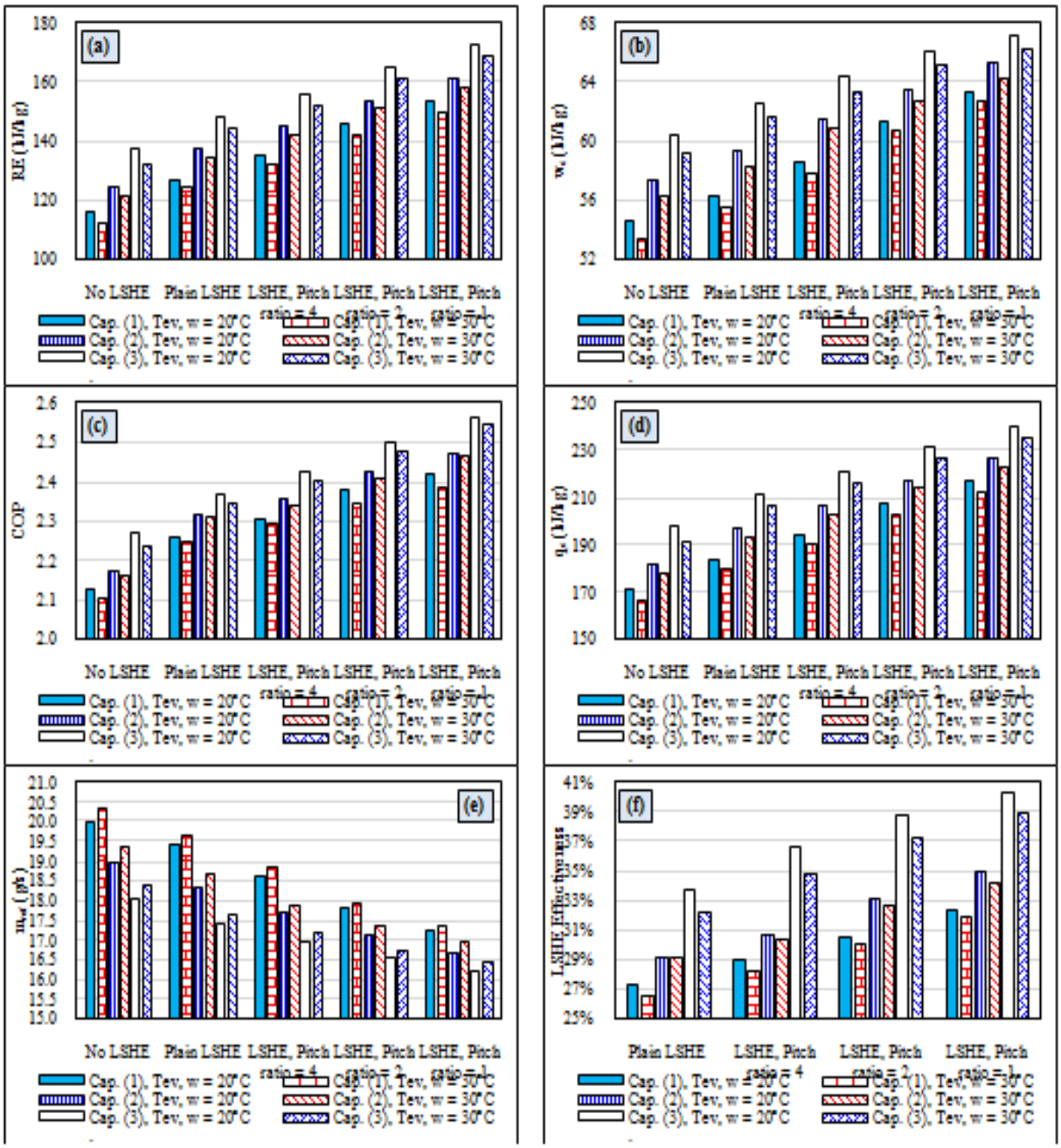

Fig. 7: Effect of LSHE characteristics on VCRS specifications; (a) RE, (b) w_{com}, (c) COP, (d) q_c, (e) m_{ref}, (f) ε_{HE}.

Table 5: Effect of the LSHE characteristics on the VCRS specifications.

Specifications	Plain LSHE	LSHE, λ = 4	LSHE, λ = 2	LSHE, λ = 1
	Percentage of average variation (%) compared with no LSHE			
RE	9.7	+15.9	+23.4	+29.4
w_{com}	+3.6	+7.4	+11.2	+14.0
COP	+5.9	+7.9	+11.1	+13.6
q_c	+7.8	+13.2	+19.6	+24.6
$\dot{m}_{ref}$	–3.5	–6.9	–10.1	–12.4
Percentage of average variation (%) compared with Plain LSHE				
ε_{HE}	———	+6.6	+13.7	+19.3

5.3 Effect of VCRS Pressures Ratio

In this analysis, the effect of the condenser to evaporator pressure ratio (P_c/P_{ev}) on the VCRS operating conditions and specifications are investigated. The P_c/P_{ev} values are varied by using three capillary tubes with different internal diameters in addition to two different temperatures of the heating water supplied to the evaporator as revealed in Table 2.

5.3.1 Effect of VCRS Pressures Ratio on VCRS Operating Conditions

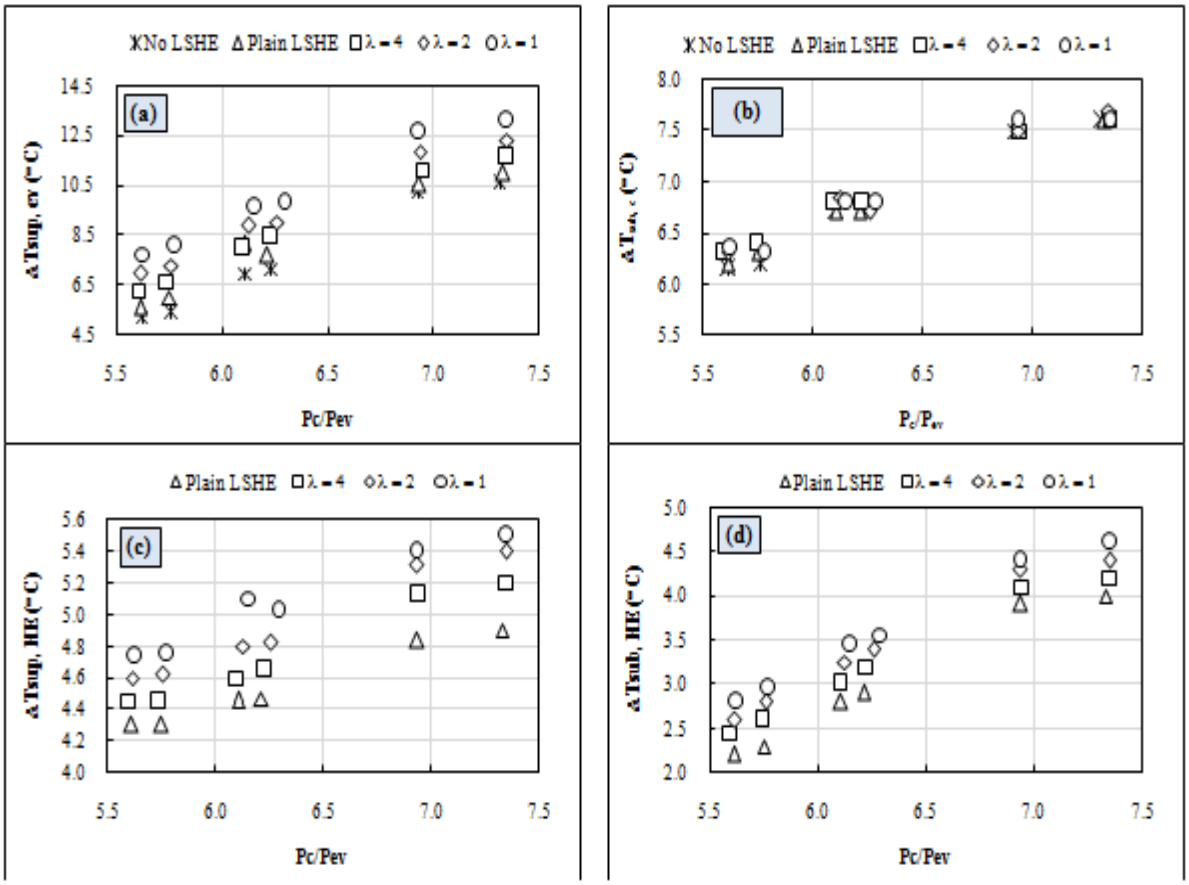

Fig. 8: Effect of VCRS pressure ratio on the cycle operating conditions; (a) $\Delta T_{sup,ev}$, (b) $\Delta T_{sub,c}$, (c) $\Delta T_{sup,HE}$, (d) $\Delta T_{sub,HE}$.

Table 6: Effect of VCRS pressure ratio on the cycle operating conditions.

Specifications	Average value for all experiments	
	P_c/P_{ev} = 5.6	P_c/P_{ev} = 7.3
$\Delta T_{sup, ev}$ (°C)	6.4	11.7
$\Delta T_{sup, HE}$ (°C)	4.5	5.3
$\Delta T_{sub, c}$ (°C)	6.3	7.6
$\Delta T_{sub, HE}$ (°C)	2.5	4.3

It is also demonstrated that the VCRS pressure ratio significantly affects the VCRS operating conditions. It is clear that increasing the VCRS pressure ratio enhances the amount of the refrigerant superheating in both the evaporator and the LSHE in addition to enhancing the amount of the refrigerant subcooling in both the condenser and the LSHE as illustrated in Table 6. In the present study, the increase in the cycle pressure ratio is due to the higher reduction in the evaporator pressure than that in the condenser. This low pressure of the evaporator reduces its corresponding saturation temperature, which enhances the rate of the heat exchange with the heating water, and consequently augments the amount of the superheating in the evaporator. Nevertheless, the refrigerant still relatively colder, which enhances the amount of superheating and subcooling in both sides of the LSHE.

In addition, although the condenser mean pressure slightly decreases, but the amount of subcooling inside the condenser is slightly increased with increasing the cycle pressure ratio. This may be due to the copper tube

connection with the LSHE, which may act as a fin. Accordingly, with increasing the rate of heat exchange in the LSHE, the subcooling inside the condenser is compensated.

5.3.2 Effect of VCRS Pressures Ratio VCRS Specifications

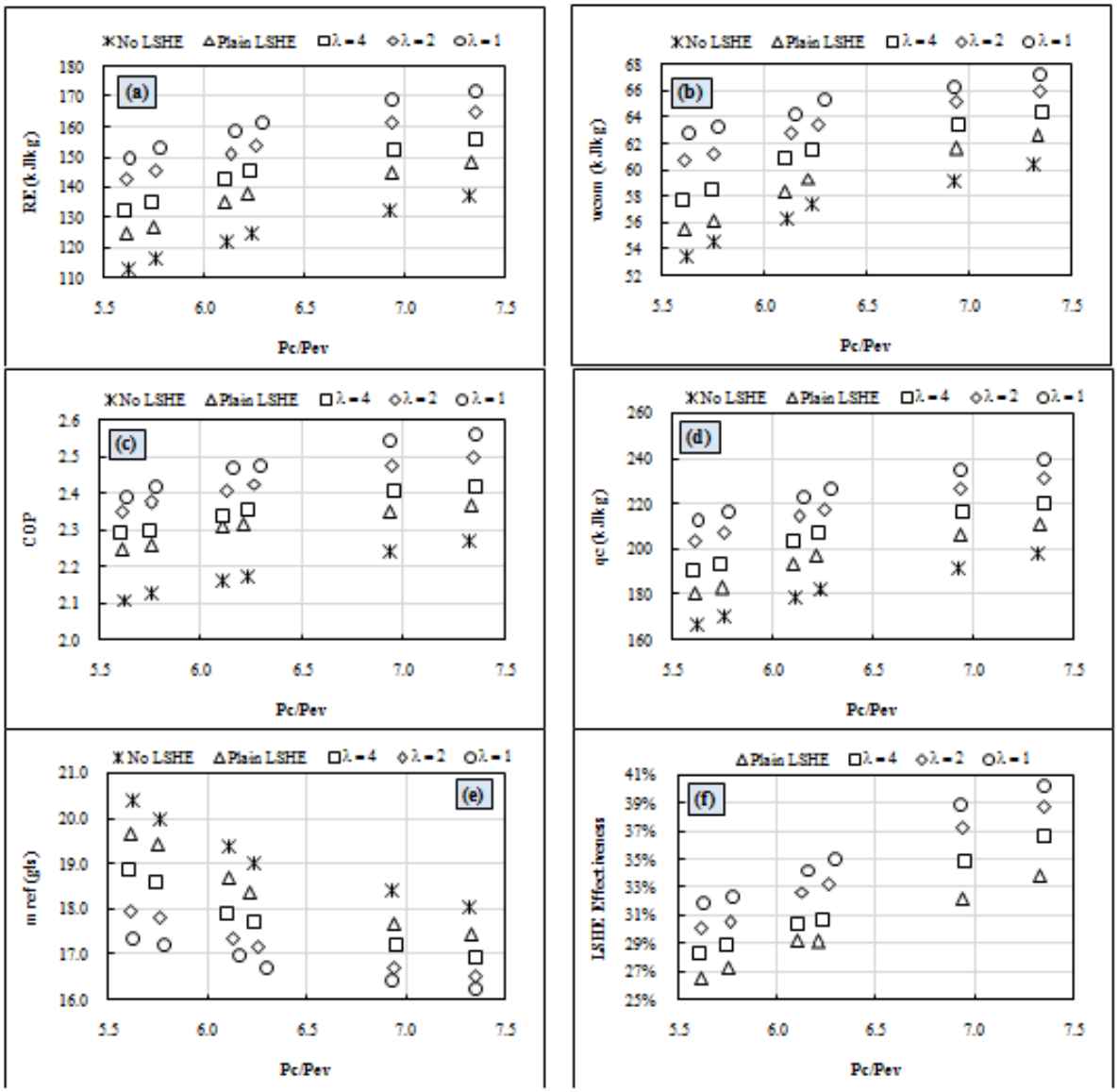

Fig. 9: Effect of VCRS compression ratio on VCRS specifications; (a) RE, (b) w_{com}, (c) COP, (d) q_c, (e) m_{ref}, (f) ε_{HE}.

Table 7: Effect of VCRS pressure ratio on the VCRS specifications.

Specifications	Percentage of average variation (%) when P_c/P_{ev} varies from 5.6 to 7.3
RE	+17.5
w_{com}	+10.4
COP	+6.5
q_c	+15.3
$\dot{m}_{ref}$	–9.6
ε_{HE}	+27.8

It is evident that increasing the VCRS pressure ratio extensively augments the evaporator refrigeration effect, compressor specific work, COP of the VCRS and the condenser heat load as illustrated in Table 7. The increase in the RE, q_c and ε_{HE} may be due to increasing the amount of superheating in the evaporator in addition to the amount of superheating and subcooling inside the LSHE, which are increased with increasing the VCRS pressure

ratio. Furthermore, the increase in the specific work of the compressor may be due to increasing the refrigerant specific volume at the compressor inlet as a result of increasing the refrigerant superheating at the compressor inlet.

6. Empirical Correlations

Using the present experimental data, empirical correlations are developed to calculate the COP of the VCRS and the effectiveness of LSHE as follows;

$$COP = 1.41\left(1+\chi\left[1+\frac{1}{\lambda}\right]\right)^{0.112}\left(\frac{P_c}{P_{ev}}\right)^{0.235} \quad (14)$$

$$\varepsilon_{HE} = 0.039\left(1+\chi\left[1+\frac{1}{\lambda}\right]\right)^{0.426}\left(\frac{P_c}{P_{ev}}\right)^{0.94} \quad (15)$$

Where χ is a constant; $\chi = 0$ for VCRS without LSHE, and $\chi = 1$ for VCRS with LSHE. Equations (14) and (15) are applicable for a VCRS based on a single stage compression unit, uses R134a as the refrigerant, with/without LSHE; $\lambda = \infty$ for a plain internal tube and $1 \le \lambda \le 4$, for a dimpled internal tube. Furthermore, these equations are valid for operating conditions of $1.79\ bar \le P_{ev} \le 2.75\ bar$, $13.73\ bar \le P_c \le 14.68\ bar$, which corresponds to $5.6 \le (P_c/P_{ev}) \le 7.3$. Comparisons of the COP of the VCRS and the effectiveness of the LSHE (ε_{HE}) with those calculated by the proposed correlations (14) and (15) are shown in Fig. 10.

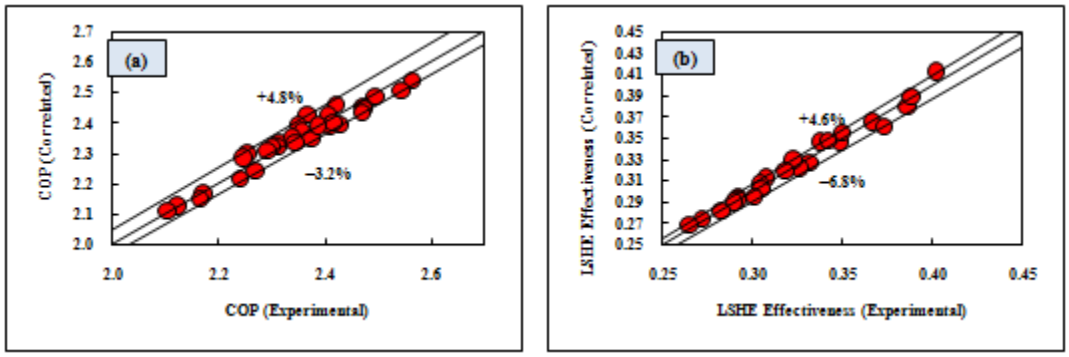

Fig. 10: Comparisons of the present experimental values with those correlated by Eqs. (14) and (15), (a) COP, (b) ε_{HE}.

From these figures, it is evident that the proposed correlations are in good agreement with the present experimental data. It is can be seen that the data falls of the proposed equations within maximum deviations of $\pm 4.8\%$ and $\pm 6.8\%$ for the COP and the effectiveness of the LSHE, respectively.

7. Conclusions

The present study investigates experimentally the effect of employing a plain/dimpled internal tube LSHE in addition to the VCRS pressure ratio on the performance characteristics of a simple VCRS based on a single stage compression unit. The LSHE is in a vertical position and the VCRS uses R134a as a refrigerant. The investigated operating parameters are LSHE; plain internal tube and dimpled internal tube of $1 \le \lambda \le 4$, $1.79\ bar \le P_{ev} \le 2.75\ bar$, $13.73\ bar \le P_c \le 14.68\ bar$, corresponds to $5.6 \le (P_c/P_{ev}) \le 7.3$. According to the results obtained here, the following conclusions can be drawn:

1. Incorporating a plain or dimpled internal tube LSHE in the VCRS considerably enhances the COP of the VCRS.
   - 1.1 Decreasing the dimples pitch ratio augments the COP of the VCRS and the LSHE effectiveness
   - 1.2 Compared with the simple VCRS, the maximum enhancement in the COP of the VCRS reaches 14% at $\lambda = 1$.
   - 1.3 Compared with the VCRS with plain LSHE, the maximum enhancement in the LSHE effectiveness is 19.3% at $\lambda = 1$.
2. Increasing the VCRS pressure ratio considerably augments the COP of the VCRS and the LSHE effectiveness; that are enhanced by 6.5% and 27.8%, respectively, with increasing the pressure ratio from 5.6 to 7.3.
3. Experimental correlations are developed to calculate the COP of the VCRS in addition to the effectiveness of the LSHE.

References

[1] N. Q. Minh, N. J. Hewitt, and P. C. Eames, "Improved Vapour Compression Refrigeration Cycles: Literature Review and their Application to Heat Pumps", International Refrigeration and Air Conditioning Conference at Purdue, July 17–20, 2006.

[2] A.O. Elsayed, "Experimental Study on the Performance of Twisted Capillary Tube", International Refrigeration and Air Conditioning Conference at Purdue, July 17–20, 2006.

[3] M. A. Akintunde, "Effect of Coiled Capillary Tube Pitch on Vapour Compression Refrigeration System Performance", AU J.T., Vol. 11(1), pp. 14–22, 2007.

[4] M. K. Khan, R. Kumar and P. K. Sahoo, "An Experimental Study of the Flow of R-134a inside an Adiabatic Spirally Coiled Capillary Tube", International Journal of Refrigeration, Vol. 31, 970–978, 2008.

[5] A. Poolkrajang and N. Preamjai, "Optimization of Capillary Tube in Air Conditioning System", Asian Journal on Energy and Environment, Vol. 10(3), 165-175, 2009.

[6] M. K. Mittal, R. Kumar, and A. Gupta, "An Experimental Study of the Flow of R-407C in an Adiabatic Spiral Capillary Tube", Journal of Thermal Science and Engineering Applications, Vol. 1, 041003-1, 2009.

[7] M. K. Mittal, R. Kumar, and A. Gupta "An Experimental Study of the Flow of R- 407C in an Adiabatic Helical Capillary Tube", Department of Mechanical and Industrial Engineering, Indian Institute of Technology, Roorkee 247667, India, International Journal of Refrigeration, Vol., pp. 33, 840 – 847, 2010.

[8] S. V. Rao, H. Sharma, P. K. Gound, T. W. and S. Gavas, "Experimental Verification of Performance of Capillary Tube Using Vapour Compression Refrigeration System", International Journal of Research in Science & Engineering, Vol. 3(2), pp. 511-516, 2017.

[9] N. Subramani and M. J. Prakash, "Experimental Studies on a Vapour Compression System Using Nanorefrigerants", International Journal of Engineering, Science and Technology, Vol. 3(9), pp. 95-102, 2011.

[10] I. M. Mahbubul, R. Saidur and M. A. Amalinaa, "Heat Transfer and Pressure Drop Characteristics of Al2O3-R141b Nanorefrigerant in Horizontal Smooth Circular Tube", Procedia Engineering, Vol. 56, pp. 323-329, 2013.

[11] R. R. Kumar, M. Narasimha and K. Sridhar, "Heat Transfer Enhancement in Air Conditioning System Using Nanofluids", International Journal of Research in Computer Application & Management, Vol. 3(5), pp. 120-126, 2013.

[12] K. Singh and K. Lal, "An Investigation into the Performance of a Nanorefrigerant (R134a+Al2O3) Based Refrigeration System", International Journal of Research in Mechanical Engineering & Technology, Vol. 4(2), pp. 158-162, 2014.

[13] T. Coumaressin and K. Palaniradja, "Performance Analysis of a Refrigeration System Using Nano Fluid", International Journal of Advanced Mechanical Engineering, Vol. 4(5), pp. 521-532, 2014.

[14] V. P. S. Kumar, A. Baskaran and K. M. Subaramanian, "A Performance Study of Vapour Compression Refrigeration System using ZrO2 Nano Particle with R134a and R152a", International Journal of Scientific and Research Publications, Vol. 6(12), pp. 410-421, 2016.

[15] V. P. Mohod and N. W. Kale, "Experimental Analysis of Vapour Compression Refrigeration System Using Nanorefrigerant", Proceedings of 68th IRF International Conference, 29th January 2017, Pune, India.

[16] T. Kanthimathi, A. Teja and D. P. Saradhi, "Enhancement of Heat Transfer Using Nano-Refrigerant", International Journal of Pure and Applied Mathematics, Vol. 115(7), pp. 349-354, 2017.

[17] S. A. Klein, D. T. Reindl and K. Brownell, "Refrigeration System Performance Using Liquid-Suction Heat Exchangers", International Journal of Refrigeration, Vol. 23(8), pp. 588-596, 2000.

[18] J. Navarro-Esbrí, R. Cabello and E. Torrella, "Experimental Evaluation of the Internal Heat Exchanger Influence on a Vapour Compression Plant Energy Efficiency Working with R22, R134a and R407C", Energy, Vol. 30(5), pp. 621-636, 2005.

[19] S. J. Inamdar and H. S. Farkade, "Performance Enhancement of Refrigeration Cycle by Employing a Heat Exchanger", International Journal of Engineering Research and Advanced Technology, Vol. 2(11), 2016.

[20] S. Inamdar and H. S. Farkade, "Performance Enhancement of Refrigeration Cycle by Employing a Heat Exchanger", International Journal of Innovative Research in Science, Engineering and Technology, Vol. 6(6), 2017.

[21] M. A. Saleh and H. E. Abdel Hameed, "Experimental/Numerical Study on Flow and Heat Transfer Performance of Dimple Interface Heat Exchanger", Zagazig University, Egypt. Vol. 18, pp. 17-72, 2010.

[22] S. Suresh, M. Chandrasekar and S. C. Sekhar, "Experimental Studies on Heat Transfer and Friction Factor Characteristics of CuO/Water Nanofluid under Turbulent Flow in a Helically Dimpled Tube", Experimental Thermal and Fluid Science, Vol. 35(3), pp. 542-549, 2011.

[23] A. A. Luki and M. Ganesan, "Flow Analysis and Characteristics Comparison of Double Pipe Heat Exchanger Using Enhanced Tubes", International Conference on Recent Trends in Engineering and Management, IOSR Journal of Mechanical and Civil Engineering, pp. 16-21, 2014.

[24] P. P. Parekh and N. K. Chavda, "Experimental and Exergy Analysis of a Double Pipe Heat Exchanger for Parallel Flow Arrangement", Parth P. Parekh International Journal of Engineering Research and Applications Vol. 4(7-2), pp. 9-13, 2014.

[25] Y. D. Banekar, S. R. Bhegade, and M. V. Sandbhor, "Dimple Tube Heat Exchanger", International Journal of Science, Engineering and Technology Research, Vol. 4(5), pp. 1632-1635, 2015.

[26] I. P. Nascimento and E. C. Garcia, "Heat Transfer Performance Enhancement in Compact Heat Exchangers by using Shallow Square Dimples in Flat Tubes, Applied Thermal Engineering, Vol. 96, pp. 659-670, 2016.

[27] A.I. Ambesange, S. S. Raut and T. C. Jagtap, "Experimental Investigation of Heat Transfer Enhancement from Dimpled Pin Fin", International Journal of Engineering Development and Research, Vol. 5(1), pp. 395-412, 2017.

[28] R. K. Ali, "Augmentation of Heat Transfer from Heat Source Placed Downstream a Guide Fence: An Experimental Study", Experimental Thermal and Fluid Science, Vol. 33, pp. 728–734, 2009.

[29] H. A. Refaey, A. A. Abdel-Aziz, R. K. Ali, H. E. Abdelrahman and M. R. Salem, "Augmentation of Convective Heat Transfer in the Cooling Zone of Brick Tunnel Kiln using Guide Vanes: An Experimental Study", International Journal of Thermal Sciences, Vol. 122, pp. 172-185, 2017.

Nomenclatures

d	Diameter, m
h	Specific enthalpy, kJ/kg
h*	Specific enthalpy in VCRS with LSHE, kJ/kg
H	Height, m
I	Electrical current, Amp
L	Length, m
ṁ	Mass flow rate, kg/s
P_{ic}	Pitch, m
P	Pressure, Pa
q	Heat per kg, kJ/kg
Q	Heat transfer rate, W
T	Temperature, ℃
T*	Temperature in VCRS with LSHE, ℃
V	Voltage drop, Volt
w	Specific work, kJ/kg
W	Power, W

Greek Letters

Δ	Differential
ε	Effectiveness
Ø	Power factor
λ	Dimple pitch to dimple diameter ratio
π	Pi ≡ A mathematical constant ≅ 3.1416
χ	A constant in Eqs. (14) and (15)

Superscripts and Subscripts

ave	Average
c	Condenser
com	Compressor
d	Dimple
ev	Evaporator

HE	Heat exchanger
HP	High pressure
i	Inner or inlet
in	Internal
LP	Low pressure
o	Out or outer
ref	Refrigerant
sub	Subcooled/subcooling
sup	Superheated/superheating
t	Tube
w	Water

Abbreviations

CAP	Capillary
COP	Coefficient of Performance
LSHE	Liquid-Suction Heat Exchanger
RE	Refrigeration effect